Original Article

MOLECULAR METABOLISM

Discovery of a potent GIPR peptide antagonist that is effective in rodent and human systems

Bin Yang [1], Vasily M. Gelfanov [1], Kimberley El [2], Alex Chen [2], Rebecca Rohlfs [1], Barent DuBois [1], Ann Maria Kruse Hansen [3], Diego Perez-Tilve [4], Patrick J. Knerr [1], David D'Alessio [2], Jonathan E. Campbell [2], Jonathan D. Douros [1,*], Brian Finan [1,*]

ABSTRACT

Objective: Glucose-dependent insulinotropic polypeptide (GIP) is one of the two major incretin factors that regulate metabolic homeostasis. Genetic ablation of its receptor (GIPR) in mice confers protection against diet-induced obesity (DIO), while GIPR neutralizing antibodies produce additive weight reduction when combined with GLP-1R agonists in preclinical models and clinical trials. Conversely, GIPR agonists have been shown to promote weight loss in rodents, while dual GLP-1R/GIPR agonists have proven superior to GLP-1R monoagonists for weight reduction in clinical trials. We sought to develop a long-acting, specific GIPR peptide antagonist as a tool compound suitable for investigating GIPR pharmacology in both rodent and human systems.

Methods: We report a structure—activity relationship of GIPR peptide antagonists based on the human and mouse GIP sequences with fatty acid-based protraction. We assessed these compounds *in vitro*, *in vivo* in DIO mice, and *ex vivo* in islets from human donors.

Results: We report the discovery of a $GIP_{(5-31)}$ palmitoylated analogue, [N^{α}-Ac, L14, R18, E21] $hGIP_{(5-31)}$-K11 (γE-C16), which potently inhibits *in vitro* GIP-mediated cAMP generation at both the hGIPR and mGIPR. *In vivo*, this peptide effectively blocks GIP-mediated reductions in glycemia in response to exogenous and endogenous GIP and displays a circulating pharmacokinetic profile amenable for once-daily dosing in rodents. Co-administration with the GLP-1R agonist semaglutide and this GIPR peptide antagonist potentiates weight loss compared to semaglutide alone. Finally, this antagonist inhibits GIP- but not GLP-1-stimulated insulin secretion in intact human islets.

Conclusions: Our work demonstrates the discovery of a potent, specific, and long-acting GIPR peptide antagonist that effectively blocks GIP action *in vitro*, *ex vivo* in human islets, and *in vivo* in mice while producing additive weight-loss when combined with a GLP-1R agonist in DIO mice.

Keywords Peptide antagonist; GIP/GIPR; GLP-1/GLP-1R; Obesity; Diabetes

1. INTRODUCTION

Glucose-dependent insulinotropic polypeptide (GIP) and glucagon-like peptide-1 (GLP-1) are incretin hormones that are secreted from enteroendocrine cells in response to nutrient stimuli and subsequently potentiate insulin secretion. The insulinotropic effect of both peptides is diminished in type 2 diabetic patients and rodents with deletion of either receptor display protection from diet-induced obesity (DIO) [1—3]. However, GLP-1 receptor (GLP-1R) agonists have been shown to effectively treat both diabetes and obesity, precipitating further interest in clinical incretin pharmacology. On the other hand, pharmacologic GIP receptor (GIPR) agonism in mice improves glucose control at the level of the islet and reduces body weight via a central nervous system mediated reduction in food intake [4]. Observations like these motivated development of next generation incretin therapies, most notably the dual the GLP-1R/GIPR agonist tirzepatide [5—8]. Conversely, emerging data from industrial drug discovery programs demonstrate that pharmacologic GIPR antagonism using neutralizing antibodies can enhance the weight-lowering efficacy of GLP-1R agonists in rodents and non-human primates [9,10]. To reconcile the observation that both GIPR agonism and antagonism can add to weight loss induced by GLP-1R agonists, it has been proposed that chronic GIPR agonism facilitates ligand-mediated receptor desensitization, thereby functionally antagonizing the GIPR [9]. This proposed requires more investigation, particularly given GLP-1R agonism has also been shown to drive receptor internalization and de-sensitization to subsequent agonist stimulation [11], but is unlikely a contributing mechanism to the clinical effectiveness of GLP-1R agonists. Nonetheless, this unified explanation for the similar directionality for GIPR agonists and antagonists on weight-loss has prompted the wider question of which approach is most beneficial in obese subjects. To that end, we sought to develop a GIPR peptide antagonist that could serve as a tool compound for interrogating this biology across species. Further elucidation of the mechanisms by which GIPR regulates body weight using this compound may serve as a foundation for developing anti-obesity therapeutics.

[1]Novo Nordisk Research Center Indianapolis, Indianapolis, IN 46241, USA [2]Duke Molecular Physiology Institute, Duke University, Durham, NC, 27705, USA [3]Global Research Technology, Novo Nordisk A/S, Måløv, Denmark [4]Department of Medicine, University of Cincinnati, Cincinnati, OH 45267, USA

*Corresponding authors. E-mails: JODQ@novonordisk.com (J.D. Douros), BFIN@novonordisk.com (B. Finan).

Received August 26, 2022 • Revision received November 8, 2022 • Accepted November 8, 2022 • Available online 15 November 2022

https://doi.org/10.1016/j.molmet.2022.101638

Abbreviations Used

Ac	Acetic acylation
ACN	Acetonitrile
BW	Body weight
cAMP	Cyclic adenosine monophosphate
C16	Palmitic acid (hexadecanoic acid)
C18-OH	Octadecanedioic acid
DCM	dichloromethane
DEPBT	Diethyl 3,4-dihydro-4-oxo-1,2,3-benzotriazin-3-yl phosphate
DIC	*N*, *N*′-Diisopropylcarbodiimide
DIEA	*N*,*N*-Diisopropylethylamine
DIO	Diet-induced obese
DMF	*N*,*N*-Dimethylformamide
γE	Gamma glutamic acid
GIP	Glucose-dependent insulinotropic peptide
GIPR	Glucose-dependent insulinotropic peptide receptor
GLP-1R	Glucagon-like peptide-1 receptor
GTT	Glucose tolerance test
hGIP	human GIP
hGIPR	human GIP receptor
HOBT	Hydroxybenzotriazole
IPGTT	Intraperitoneal glucose tolerance test
mGIP	mouse GIP
mGIPR	mouse GIP receptor
OEG	8-amino-3,6-dioxaoctanoic acid (AEEA)
OGTT	Oral glucose tolerance test
Pla	L-(−)-3-phenyllactic acid/L-3-phenyllactic acid/S-3-phenyllactic acid
Mtt	4-Methyltrityl
TFA	Trifluoroacetic acid
Tis	Triisopropylsilane

Previously, N-terminal or C-terminal truncated GIP fragments were systematically studied for GIPR binding and cAMP signal transduction [12]. (Pro3)GIP and N- or C-terminally truncated fragments including $GIP_{(3-30)}$, $GIP_{(5-30)}$, $GIP_{(6-30)}$, $GIP_{(3-42)}$, and $GIP_{(5-42)}$ have been studied for their antagonistic effects on GIPR-mediated insulin release, insulin resistance, glucose control, lipid metabolism, and body weight regulation [13–15]. However, these GIP fragments demonstrated variable profiles of antagonism and agonism *in vitro.* These candidates frequently suffer from a lack of potency, partial antagonism, residual agonism at the GIPR, and cross-reactivity to GLP-1R [13,16–21]. In particular, the widely used $hGIP_{(3-30)}$ is known to potently inhibit primate GIPRs *in vitro* [22], and effectively block GIPR action in clinical studies [23]. However, the lack of acylated protraction (i.e. relatively short circulating half-life) makes this compound unamenable to chronic dosing studies. In this report, we present a condensed structure activity relationship (SAR) campaign which culminates in the discovery of a potent, acylated GIPR peptide antagonist [N^{α}-Ac, L14, R18, E21]$hGIP_{(5-31)}$- K11 (γE-C16) (referred to herein as **7**). This compound contains amino acid mutations and a fatty monoacid acylation, both of which directly contribute to its potency for antagonizing GIP-induced cAMP signaling at the hGIPR and mGIPR. Additionally, this GIPR peptide antagonist reduced GIP-induced glycemic control in mice and enhanced weight loss when chronically co-administrated with semaglutide in DIO mice. The latter phenomenon has previously only been demonstrated with GLP-1 agonists and GIPR antibody combinations. Further, the described antagonist reduced GIP-, but not GLP-1, mediated insulin secretion in intact islets from human donors. This peptide antagonist represents a research tool that is amenable for the study of GIP biology across a variety of experimental paradigms and will fuel discovery efforts for next generation peptide-based GIPR antagonists.

2. METHODS

2.1. Peptide synthesis

Peptides were synthesized by automated Fmoc/tBu solid-phase methodology employing a Symphony X peptide synthesizer (Gyros Protein Technologies, Tucson, AZ) or an ABI 431 A peptide synthesizer (Applied Biosystems, Foster City, CA). Peptides bearing a C-terminal acid were assembled using preloaded Wang-polystyrene resin (AAPPtec, Louisville, KY; Novabiochem, San Diego, CA), and peptides bearing a C-terminal amide were assembled using H-Rink Amide ChemMatrix® resin (PCAS BioMatrix Inc, Saint-Jean-sur-Richelieu, Quebec, Canada). All Fmoc-amino acids and synthesis reagents were purchased from Midwest Biotech (Fisher, IN), AAPPtec, or Gyros Protein Technologies unless otherwise specified. Fmoc-amino acids were coupled at tenfold excess relative to resin loading with 6-chloro-1-hydroxybenzotriazole (6-Cl-HOBt)/*N*,*N*′-diisopropylcarbodiimde (DIC) or OxymaPure (ethyl 2-cyano-2-(hydroxyimino)acetate)/DIC activation in *N*,*N*-dimethylformamide (DMF). The Fmoc protecting group was removed with 20% piperidine in DMF. N-terminal acetylation was performed on-resin with tenfold excess of acetic anhydride/*N*,*N*-diisopropylethylamine (DIEA) in dichloromethane (DCM) for 1 h. N-terminal L-3-phenyllactic acid (Pla) was coupled manually at 5-fold excess with diethyl 3,4-dihydro-4-oxo-1,2,3-benzotriazin-3-yl phosphate (DEPBT)/DIEA activation in DMF. N^{α}-Boc protection was coupled with Boc-ON in DMF/DIEA.

For peptides bearing fatty acid modifications, Fmoc-L-Lys (Mtt)-OH was incorporated at the position to be modified during assembly of the peptide backbone. Following incorporation of either acetic capping or N^{α}-Boc protection of the N-terminal amino acid after completion of the peptide backbone, the Mtt protecting group was removed with 1–2% trifluoroacetic acid (TFA)/5% triisopropylsilane (TIS) in DCM. Components of the modification were then coupled sequentially as described above, using Fmoc-Glu-OtBu, Fmoc-8-amino-3,6-dioxaoctanoic acid, palmitic acid, and/or octadecanedioic acid mono-*tert*-butyl ester (Novo Nordisk, Måløv, Denmark) as required.

Completed peptides were cleaved from resin and globally deprotected using 5% TIS/5% H_2O in TFA for 2 h with agitation. For peptides containing cysteine and/or methionine, 2.5% 2-mercaptoethanol or 2.5% 3,6-dioxa-1,8-octanedithiol was added to the cleavage solution. The cleaved peptide in TFA were filtered, precipitated with ether, isolated by centrifugation, and dissolved in 2% acetic acid/20% acetonitrile (ACN) in water. The crude peptide solution was loaded onto a Luna 19 × 250 cm/10 μm C8 column (Phenomenex, Torrance, CA) and purified using a gradient elution of increasing ACN in aqueous 0.1% TFA on a Waters 2545 preparative HPLC system. Peptide fractions were characterized for identity and purity by liquid chromatography–mass spectrometry on an Agilent 1260 Infinity/6120 Quadrupole instrument with a Kinetex C8 column and a gradient of 10%–80% eluent B in eluent A. Eluent A is 0.05% TFA in water, and eluent B is 0.05%TFA/10% water in ACN. Peptides with purity over 95% were pooled and lyophilized.

Concentrations of aqueous peptide solutions for *in vitro* and *in vivo* evaluation were measured by UV absorption at 280 nm on a NanoDrop 1000 spectrophotometer (Thermo Scientific, Wilmington, DE). Peptide

extinction coefficients at 280 nm were calculated using tryptophan (5500 $M^{-1}cm^{-1}$) and tyrosine (1490 $M^{-1}cm^{-1}$) content according to the manufacturer's guidelines.

2.2. In vitro potency assays

Cyclic AMP (cAMP) production was assessed as a proxy for receptor activation or antagonism using a standardized Cre-luciferase assay that has been reported previously [24,25]. In brief, stably transfected baby hamster kidney (BHK) cell lines expressing either GLP-1R, GIPR, or glucagon receptor (GcgR) and firefly luciferase reporter gene linked to the cAMP response element (CRE) were seeded in poly-D-lysine-coated 96 well opaque well tissue culture plates at 5,000 cells per well in growth media. Cells were incubated overnight then medium was removed, the plate was washed once in Dulbecco's phosphase-buffered saline (DPBS) and 50 μL of assay buffer (DMEM without phenol red, 10 mM HEPES, 1× Glutamax, 1% ovalbumin, 0.1% Pluronic F-68) containing serial dilutions of test compounds was added to each well. The compounds were serially diluted across the rows of a separate low-bind 96-well plate in assay buffer with or without EC_{80} concentration of native ligand to create a 12-point dose response curve. The test plates were incubated 3 h at 37 °C in CO_2 incubator. After the incubation, the plates were washed once with 100 ul/well DPBS followed by addition of 100 μL per well of SteadyLite plus reagent (PerkinElmer). The assay plates were covered to protect reagent from light, shaken at 250 rpm at room temperature for 30 min, and read in a microtiter plate reader. EC_{50} and IC_{50} values were calculated using Prism software (GraphPad) as the nonlinear regression of log (compound concentration) vs. response.

2.3. In vitro receptor binding assay

GIP receptors were inserted in pcDNA3 vectors under the control of the CMV promoter with Geneticin as the selection marker. Upon transfection of Baby Hamster Kidney (BHK) cells with these plasmids stable clones expressing receptor were selected in culture media containing geneticin (G418). Competitive binding of peptide antagonists to the full length GIP receptor was assessed in whole cells using radiolabeled human GIP (Tyr^{125}I-NNC0090-0554, produced at Novo Nordisk A/S). The GIP receptor expressing cells were seeded in poly-D-lysine coated white 96-well plates with clear bottom (Corning, cat. No. 354651) at 5000–10000 cells per well in DMEM medium (Life Technologies, cat. No 61965-026) supplemented with Geneticin (Life Technologies, cat. No 10131-027) and 10% fetal bovine serum (FBS) (Life Technologies, cat. No 16140-071). The following day the medium was removed, and cells were rinsed twice with HBSS (Life Technologies, cat. No 14025), then the mixture of 60 pM radiolabeled GIP with serial 10-fold dilutions of test compounds in the binding assay buffer was added in duplicate. The assay buffer consisted of HBSS (Life Technologies, cat no 14025), 10 mM HEPES (Life Technologies, cat. No 15630), 0.1% pluronic F-68 (Life Technologies, cat. No 2404) and 0.1% ovalbumin (Sigma–Aldrich, cat. No A5503) pH 7.4. The plate was sealed and incubated at 4 °C overnight. The supernatant was discarded, and the plates were washed twice with ice cold PBS (Life Technologies, cat. No 14040-091). The cells were lysed with 50 μl per well 0.1 M NaOH followed by 5 min shaking. One hundred μl microscint-40 (Perkin Elmer, cat. No 6013641) was added to each well, and after 30 min incubation at room temperature, the plates were counted in a scintillation counter. Nonlinear regression analysis was performed in GraphPad Prism 9 (GraphPad software, USA) using non-linear three parameter regression of log (inhibitor concentration) vs response. Data were reported as geometric mean of IC_{50} values with 95% CI.

2.4. In vivo studies in mice

2.4.1. Animal studies

All mice studies were performed in accordance Institutional Animal Care and Use Committee guidelines at University of Cincinnati. Male C57BL/6 J mice (Jackson Laboratories) were housed 4 per cage under 12 h/12 h light–dark cycle at 22 °C with *ab libitum* access to water and 58% fat, high-sugar diet (D12331, Research Diets) for at least 16 weeks to induce Diet-Induced Obesity (DIO).

2.4.2. Pharmacokinetic (PK) study

DIO C57BL/6 J mice (58% HFD diet, male, body weight 61–74 g), were given subcutaneous injections of peptide **7** or **13** at a single dose of 500 nmol/kg; n = 4 mice per group). Plasma was collected at time points of 5min, 30min, 1 h, 2 h, 4 h, 8 h, 24 h, 48 h, and 72 h for both peptides. To measure plasma concentration, standards of each peptide were prepared in mouse plasma ranging from 0.5 to 4000 nM. A protein precipitation was performed by organic solvent extraction with a 14-fold dilution with methanol. The samples were centrifuged for 20 min at 4 °C at 13 000 g-force. Supernatants of samples were collected and diluted 3-fold with 0.1% formic acid in water. The diluted samples were then subjected to LC-MS analysis on a Thermo Q Exactive HF mass spectrometer interfaced with a Vanquish UPLC. LC separations were performed on an Acquity UPLC BEH C18 1.7 μm, 1.0 × 50 mm column. Mobile phase A was composed of 0.1% formic acid in water and mobile phase B was composed of 0.1% formic acid in acetonitrile. The LC flow rate was set to 0.4 μL/min using a gradient elution from 10 to 95% B over the course of 4.0 min. Selected ion monitoring was used for both molecules, where the 3+ ion, 1212.6807 *m/z*, and the 5+ ion, 1017.1634 *m/z*, were chosen for peptides **7** and **13**, respectively. Plasma data were analyzed by non-compartmental methods with sparse sampling using Phoenix WinNonlinTM 8.3.

2.4.3. Intraperitoneal and oral glucose tolerance testing

For intraperitoneal glucose tolerance tests (IPGTT) and oral glucose tolerance tests (OGTT), animals were fasted for 6 h prior to glucose injection with access to water. Baseline tail-vein blood glucose was measured, then mice were injected i.p. or gavaged orally with 2.5 g/kg of 20% glucose solution (12uL/g). For GTTs with either GIPR or GLP-1R agonists, animals were injected with the GIPR antagonist (500 or 1500 nmol/kg) 2 h prior to glucose administration and 1 nmol/kg acyl-GIP or 2 nmol/kg semaglutide 1 h prior to glucose administration.

2.4.4. Pharmacodynamic effects of GIPR antagonists on body weight

DIO male C57BL/6 J mice (body weight 55 g, n = 8 per group Jackson Laboratories) were housed 4 per cage under 12 h/12 h light–dark cycle at 22 °C with *ab libitum* access to water and 58% fat, high-sugar diet (D12331, Research Diets) for ∼12 weeks. Mice achieved body weight (BW) greater than 55 g on average and were subsequently assigned to treatment groups (n = 8 per group) which were normalized for body weight. Treatment groups received either vehicle, semaglutide (2 nmol/kg/d), GIPR antagonist (500 or 1500 nmol/kg/d), semaglutide + GIPR antagonist (2 nmol/kg/d + 500 or 1500 nmol/kg/d; co-formulated single injection). Test compounds (200uM) were dissolved in a vehicle (pH 7.4) containing 0.05% polysorbate-80, 50 mM sodium phosphate, and 70 mM sodium chloride; test compounds were administered once daily for 28 days, subcutaneously during the light cycle at a volume of 3.9 μL/g BW.

Body weight and food intake were measured prior to dosing every other day; the percent change in body weight was calculated for each mouse based on its initial body weight. Food intake was measured on a per cage basis (n = 2 cages/group) and normalized to the number of mice (4/cage). Tail blood glucose levels were measured 0, 15, 30, 60, 90, and 120 min following the glucose load. An additional measure of 6 h fasting insulin (Crystal Chem 90080), resistin (R&D Systems MRSN00), CTX (Novus Biologicals NBP2-69074) and total GIP (Crystal Chem 81527) levels were taken at d28.

2.5. Human islet provision

Human islets for research were provided by the Alberta Diabetes Institute Islet Core at the University of Alberta in Edmonton (www.bcell.org/adi-isletcore) with the assistance of the Human Organ Procurement and Exchange (HOPE) program, Trillium Gift of Life Network (TGLN), and other Canadian organ procurement organizations. Islet isolation was approved by the Human Research Ethics Board at the University of Alberta (Pro00013094). Further details on this protocol can be found at the aforementioned website. All donors' families gave informed consent for the use of pancreatic tissue in research. Prep purity for procured islets was at least 80%. Human islets were received and processed same day. They recovered overnight in RPMI [6.7 mM glucose, 10 mM HEPES, 100 U/mL penicillin, 100 ug/mL streptomycin, 0.25 ug/mL Amphotericin B (Gibco), and 10% FBS] and used within 4 days in perifusion.

2.6. Human islet perifusion

After recovery, 75 islets were handpicked and placed into chambers containing 2.7 mM glucose Krebs-Ringer-phosphate-HEPES (KRPH) buffer [140 mM NaCl, 4.7 mM KCl, 1.5 mM $CaCl_2$, 1 mM NaH_2PO_4, 1 mM $MgSO_4$, 2 mM $NaHCO_3$, 5 mM HEPES] and 1% FA-free BSA (pH 7.4) with 100 uL of Bio-Gel P-4 Media (Bio-Rad). Islets were equilibrated for 48 min (24 min at 1% BSA, 24 min at 0.1% BSA) and then perifused in intervals based on the experimental conditions. GIPR antagonist (1 uM), GIP (30 nM), and GLP-1 (30 nM) were prepared in KRPH buffer + 0.1% BSA. Islet proteins were extracted in acid ethanol to assess total insulin and glucagon levels. Hormone secretion of insulin and glucagon was assayed with Lumit Immunoassay Kits (Promega, CS3037A02, respectively) and measured using the EnVision plate reader (PerkinElmer).

3. RESULTS

3.1. Truncated $GIP_{(3-30)}$, $GIP_{(5-31)}$, and $GIP_{(6-31)}$ fragments act as GIPR inhibitors

Truncated $hGIP_{(3-30)}$ amide has been shown to antagonize both human and rodent GIPRs in transfected cell lines and primary adipocytes [22,26]. Therefore, we began our SAR campaign (Table 1) using this foundational backbone. We show that GIP-mediated cAMP accumulation is reduced by $hGIP_{(3-30)}$ amide (**1**) by 81% at the hGIPR (IC_{50} = 64.1 nM). While maximal cAMP production is reduced by 73% at the mGIPR, there is severely limited potency at this receptor (IC_{50} = > 6000 nM; Table 1; Figure 1A,B), highlighting the species differences in GIP pharmacology. Modification of the $hGIP_{(3-30)}$ amide backbone to [L14, R18, E21] $hGIP_{(3-30)}$ amide (**2**) was chosen to aid potency at the mouse receptor (via R18) and improve physiochemical stability (via L14 and E21). Peptide **2** demonstrated improved functional potency at both hGIPR (IC_{50} = 16.2 nM) and mGIPR (IC_{50} = 543 nM; Table 1, Figure 1A,B) relative to **1**. However, the yet limited mGIPR potency of **2** presented a further opportunity to improve the pharmacological profile across mouse and human receptors. We

Table 1 — Sequences and GIPR antagonism profiles of GIP truncated derivative peptides.

Compound Name	Peptide	Sequence	cAMP IC50, nM (% inhibition)[a]		Receptor Binding IC50(nM)[b]	
			hGIPR	mGIPR	hGIPR	mGIPR
mGIP	N/A		EC_{50} = 0.01	EC_{50} = 0.017		
$hGIP_{(3-30)}$	1	EGTFISDYSIAMDKIHQQDFVNWLLAQK-NH2	64.1 (81%)	>6000 (73%)	1.55 ± 0.49	35.1 ± 16.9
[L14, R18, E21] $hGIP_{(3-30)}$	2	EGTFISDYSIALDKIRQQEFVNWLLAQK-NH2	16.2 (72%)	543 (86%)	Nd	nd
[L14, R18, E21] $hGIP_{(5-31)}$	3	TFISDYSIALDKIRQQEFVNWLLAQKG	36.4 (81%)	407 (93%)	1.80 ± 0.71	18.7 ± 6.6
[L14, R18, E21] $hGIP_{(6-31)}$	4	FISDYSIALDKIRQQEFVNWLLAQKG	176 (83%)	572 (91%)	6.45 ± 0.92	37.1 ± 6.0
[Pla6, L14, R18, E21] $hGIP_{(6-31)}$	5	PISDYSIALDKIRQQEFVNWLLAQKG	48.7 (98%)	334 (99%)	2.98 ± 1.68	22.7 ± 7.9
[L14, R18, E21] $hGIP_{(3-30)}$-K11 (γE-C16)	6	EGTFISDYKIALDKIRQQEFVNWLLAQK-NH2	3.44 (100%)	35.1 (97%)	0.36 ± 0.03	2.1 ± 0.42
[Nα-Ac, L14, R18, E21] $hGIP_{(5-31)}$-K11 (γE-C16)	7	TFISDYKIALDKIRQQEFVNWLLAQKG	0.71 (100%)	3.6 (100%)	0.35 ± 0.15	1.50 ± 0.57
[Pla6, L14, R18, E21] $hGIP_{(6-31)}$-K11 (γE-C16)	8	PISDYKIALDKIRQQEFVNWLLAQKG	1.91 (100%)	14.0 (99%)	0.50 ± 0.08	1.55 ± 0.07
[N^{α}-Ac, L14, R18, E21] hGIP(5−31)-K11 (-C18-OH)	9	TFISDYKIALDKIRQQEFVNWLLAQKG	17.2 (100%)	58.1 (100%)	0.90 ± 0.02	5.4 ± 2.12
[N^{α}-Ac, L14, R18, E21] $hGIP_{(5-31)}$-K11(OEG_2-C18-OH)	10	TFISDYKIALDKIRQQEFVNWLLAQKG	9.5 (100%)	153 (100%)	2.49 ± 1.48	8.7 ± 4.38
[N^{α}-Ac, L14, R18, E21] $hGIP_{(5-31)}$-K11(OEG_2-γE-C18-OH)	11	TFISDYKIALDKIRQQEFVNWLLAQKG	18.9 (100%)	242 (100%)	3.83 ± 2.27	24.8 ± 4.8
[N^{α}-Ac, L14, R18, E21] $hGIP_{(5-31)}$-K10 (γE-C16)	12	TFISDKSIALDKIRQQEFVNWLLAQKG	0.61 (100%)	12 (100%)	0.21 ± 0.12	1.0 ± 1.57
[N^{α}-Ac, L14, R18, E21] $hGIP_{(6-42)}$-K10 (γEγE-C16)	13	TFISDKSIALDKIRQQEFVNWLLAQKGKKNDWKHNITQ-NH2	0.48 (100%)	26.1 (100%)	0.46 ± 0.14	1.62 ± 1.1

[a] IC_{50} of inhibiting added constant GIP with 70−90% cAMP stimulation on human and mouse GIP receptors. Percentage inhibitions indicate the maximal antagonism or the antagonism up to the last testing peptide concentration.
[b] IC50 of *in vitro* receptor binding affinity on human and mouse GIP receptors. Data are average ± SD of three independent experiments or mean from one validated duplicate experiment. Ac: acetic acylation. P: 3-L-Phenyllactic acid. OEG: 8-amino-3,6-dioxaoctanoic acid (AEEA). C16: palmitic acid (hexadecanoic acid). C18-OH: octadecanedioic acid. γE: gamma-glutamic acid. Nd: not determined or not available. K: K (γE-C16), **K:** K (-C18-OH), *K:* K(OEG2-C18-OH), K: K(OEG2-γE-C18-OH), K: K (γEγE-C16), T: Ac-T.

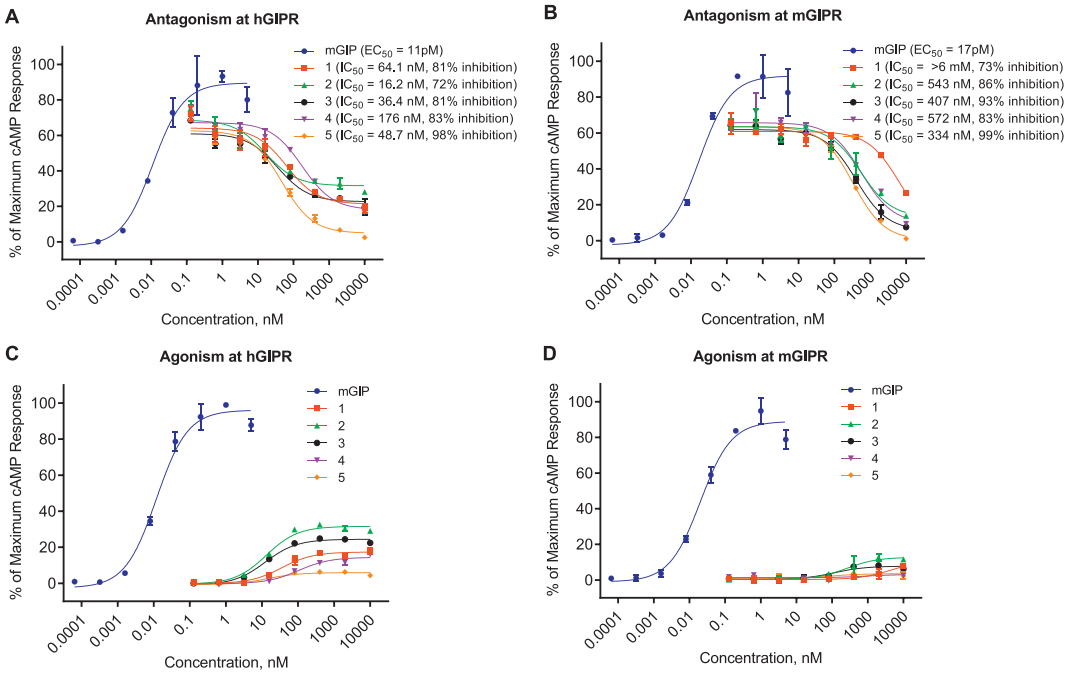

Figure 1: Truncated GIP peptides inhibit GIP-induced cAMP in hGIPR and mGIPR expressing cells. (A, B) Inhibition of GIP-induced cAMP production by $hGIP_{(3-30)}$ (**1**), [L14, R18, E21] $hGIP_{(3-30)}$ (**2**), [L14, R18, E21] $hGIP_{(5-31)}$ (**3**) and [L14, R18, E21] $hGIP_{(6-31)}$ (**4**), and [Pla6, L14, R18, E21] $hGIP_{(6-31)}$ (**5**) peptides on hGIPR (A) and mGIPR (B). (C, D) cAMP production mediated by peptide **1**–**5** at the hGIPR (C) and mGIPR (D). Data represent the mean ± SEM of duplicate experiments.

next explored slight iterations to the N- and C-terminus. The [L14, R18, E21]$hGIP_{(5-31)}$ **(3)** and [L14, R18, E21] $hGIP_{(6-31)}$ **(4)** peptide backbones showed hGIPR inhibition of 81% (IC_{50} = 36.4 nM) and 83% (IC_{50} = 176 nM) respectively, and mGIPR inhibition of 93% (IC_{50} = 407 nM) and 91% (IC_{50} = 572 nM) respectively (Table 1, Figure 1A,B). Inspired by our previous work on glucagon receptor antagonists [25], a 3-L-phenyllactic acid (Pla) mutation was used at position 6 of peptide **4** ([Pla6, L14, R18, E21] $hGIP_{(6-31)}$; **5**) and resulted in full inhibition with improved potency at hGIPR (IC_{50} = 48.7 nM) and mGIPR (IC_{50} = 334 nM) (Table 1, Figure 1A,B). While **1**, **2**, **3**, and **4** all show partial agonism at the hGIPR (Figure 1C) they show no significant agonism at the mGIPR (Figure 1D). Critically, **5** shows no significant agonism at either receptor (Figure 1C,D). The receptor binding assays (Table 1) show a similar rank ordering of potency between compounds **1**, **3**, **4** and **5** as that seen with the functional cAMP signaling assays. However, there does appear to be limited resolution between the most potent compounds, which may be due to the receptor over-expression cellular system used in the functional assays.

3.2. Acylation influences the antagonistic potency of hGIP based peptides

We next conjugated fatty acid-based protractors to the GIP fragments described above as a means to extend circulating half-life and support longer exposures necessary for *in vivo* use of these compounds. Using a similar strategy to that seen in our in our incretin agonists optimization, we mutated position 11 in **2**, **3**, and **5** to lysine and appended a palmitoyl acylation (C16 monoacid) via a single gamma-glutamic acid spacer (γE) to produce compounds **6**, **7**, and **8**, respectively. We found that this acylation improved both efficacy and potency for all compounds at both the human and mouse GIPR. This is similar to the phenomenon seen with our previous reports of protracted GIPR agonists [27]. Peptide **6** displayed antagonism and improved potency at hGIPR (IC_{50} = 3.44 nM) and mGIPR (IC_{50} = 35.1 nM) compared to the non-acylated precursor **2**. Peptide **7**, which is an acylated form of peptide **3,** showed antagonism at human and mouse GIPR and further increased potency at hGIPR and mGIPR (IC_{50} = 0.78 nM and IC_{50} = 3.98 nM, respectively Figure 2), resulting in a peptide antagonist with the requisite receptor pharmacological profile to enable feasible *in vivo* proof of concept testing. Although acylation of the Pla6-containing backbone **5** enhanced potency at both species of receptors (IC_{50} = 1.91 nM at hGIPR and IC_{50} = 14.0 nM at mGIPR), the resulting potency of **8** was less than that of **7** (Table 1, Figure 2). Peptide **7** showed more potent antagonism of GIP-stimulated cAMP production than either than peptide **6** or **8** in human and mouse GIPR over-expressing cells, indicating a unique pharmacology of the protractor beyond simple extension of time-action. However, in an *in vitro* receptor binding assay (Table 1), the three peptides show very similar binding affinity. We also assessed hGIPR and mGIPR agonism by peptides **6, 7,** and **8**. These compounds exhibited negligible cAMP production as agonists compared to native GIP (Figure 2E,F), and thus do not show aspects of residual GIPR agonism. Finally, we tested the ability of our most potent GIPR antagonist **7** to inhibit activation of the GIPR by acyl-GIP [27] (Supplementary Figure 1). We found that acyl-GIP is more potent than native GIP at both hGIPR and mGIPR. Accordingly, **7** was able to fully antagonize activation of both GIPRs by acyl-GIP (hGIPR IC_{50} = 6.27 nM, 100% inhibition, mGIPR IC_{50} = 32 nM, 100% inhibition) but at lower potency than the antagonism of native GIP.

3.3. Acylated GIPR antagonist **7** displays cross-reactivity with other class B GPCRs

It is common for truncated peptide antagonists to demonstrate promiscuity at other closely related receptors. We assessed the agonism and antagonism of **7** at the GLP-1R (Figure 3A–D) and found that it inhibited native GLP-1 action but with a considerably lower potency at the hGLP-1R (IC_{50} = 262 nM, 68% inhibition) relative to hGIPR (IC_{50} = 0.71 nM, 100% inhibition). The agonism was limited to 20%

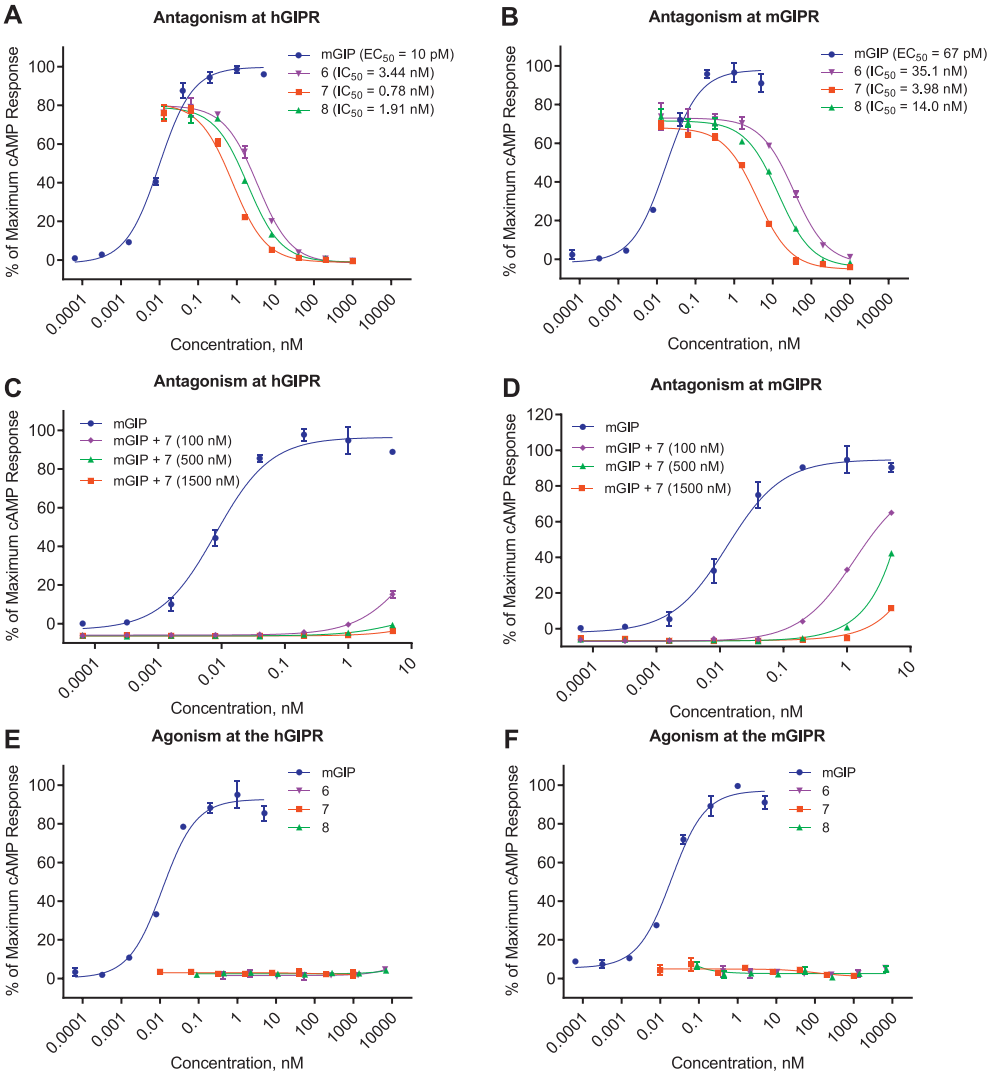

Figure 2: Acylated truncated GIP peptides inhibit GIP-induced cAMP production in hGIPR and mGIPR expressing cells. (A, B) Inhibition of GIP-induced cAMP production by **6, 7,** and **8** at the hGIPR (A) and mGIPR (B) in response to 50pM GIP. (C, D) GIP antagonism of peptide **7** in attenuating dose-dependent GIP-induced cAMP production at the hGIPR (C) and mGIPR (D). (E, F) Agonism of peptides **6**, **7** and **8** at hGIPR (E) and mGIPR (F). Data represent the mean ± SEM of a duplicate experiments.

with potency, about 4 orders of magnitude lower than GLP-1 (Figure 3C). Peptide **7** also drove less antagonism at the mGLP-1R relative to hGLP-1R. Despite this cross-reactivity at the two GLP-1Rs tested, we see little if any functional consequence of this phenomenon *in vivo* in our rodent studies (*Section 3.6*) or *ex vivo* in human islets at the doses tested (*Section 3.8*). Peptide **7** showed nominal agonism at either mGcgR ($EC_{50} = > 7$uM) or hGcgR ($EC_{50} > 12$uM), and no antagonism at the mGcgR (Figure 3E–F). While peptide **7** did display relatively potent antagonism at the hGcgR ($IC_{50} = 42$ nM). It did not diminish glucose stimulated insulin secretion from human islets [28], indicating the functionality of hGcgR antagonism is limited in the contexts assessed here (Figure 7).

3.4. Protraction type, linker, and position influence the antagonism of hGIP peptide fragments

We found that peptide **7** exhibited superior antagonism at both hGIPR and mGIPR compared to both **6** and **8** (Figure 2A,B). We next sought to understand how acylation type, linker chemistry, and position influences the antagonistic action of **7** as a means to further optimize this compound (Table 1). Inspired by long-acting GLP-1R agonists such as semaglutide [29], we began by replacing the C16 acylation with an octadecanoyl protractor bearing a terminal carboxylate (C18-OH) and explored different compositions of the linker between the peptide backbone and the protractor, with the ambition that the C18-OH protractor will enable a longer circulating half-life and greater overall exposure. Substitution of the γE-C16 acylation in **7** with C18-OH ([N^a-Ac, L14, R18, E21] $hGIP_{(5-31)}$-K11 (-C18-OH; **9**), reduced potency at hGIPR to 17.2 nM and 58.1 nM at mGIPR (Table 1). Addition of a short, PEG-based linker ([N^a-Ac, L14, R18, E21] $hGIP_{(5-31)}$-K11(OEG_2-C18-OH; **10**) improved potency at hGIPR ($IC_{50} = 9.5$ nM) but concomitantly reduced potency at mGIPR ($IC_{50} = 153$ nM; Table 1). Reintroduction of γE in the linker to generate the same acylation as semaglutide ([N^a-Ac, L14, R18, E21] $hGIP_{(5-31)}$-K11(OEG_2-γE-C18-OH; **11**) maintained relative potency at hGIPR ($IC_{50} = 18.9$ nM) but further reduced it at mGIPR ($IC_{50} = 242$ nM) (Table 1). Similar reductions in binding affinity at both hGIPR and mGIPR, correlating with functional potency, were also observed for C18-OH acylated peptides **9** to **11** compared to **7** (Table 1). Therefore, we conclude that the C18-OH

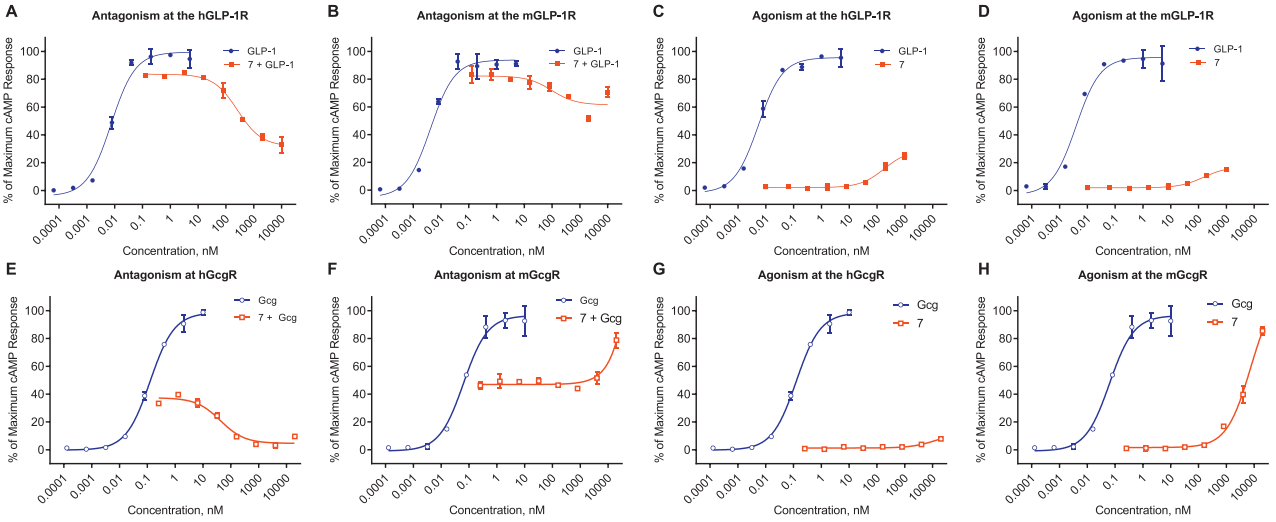

Figure 3: Peptide 7 has limited pharmacologic action at the GLP-1R, but retains antagonism at the hGcgR. Antagonistic (A, B, E, F) and agonistic (C, D, G, H) effect of **7** on cAMP signaling GLP-1 at the hGLP-1R (A, C) mGLP-1R (B, D) and glucagon (Gcg) at the hGcgR (E, G) and mGcgR (F, H). Data represent the mean ± SEM of a duplicate experiment.

protractor proves deleterious for potent GIPR antagonism compared to the C16 iterations, and such reductions in potency should be balanced with the improved pharmacokinetics predicted for C18-OH protraction. This should be taken into consideration when examining the effects seen in other reports [15]. Additionally, during our residue protraction position screening studies, specifically moving the C16 protractor from position 11 as seen in **7** to position 10 (**12**), did not significantly alter the potency at hGIPR (IC_{50} = 0.61 nM) but reduced the potency at mGIPR (IC_{50} = 12.4 nM; Table 1). Peptide **12** shows a similar antagonistic profile to our previously published position 10 acylated long peptide (**13** in Table 1**).**

3.5. Peptide **7** has a PK profile amenable to once-daily dosing in mice

The plasma PK parameters of peptides **7** and **13** were quantified after a single subcutaneous (SC) injection (500 nmol/kg) in DIO C57BL/6 J mice (Figure 4, Supplemental Figure 2). The maximum plasma concentration (C_{max}) and time to maximum concentration (t_{max}) for **7** and **13** were comparable. The total plasma exposure (AUC of 137,272 h nM) and half-life (8.45 h) for **7** were substantially greater than those of **13** (AUC of 21,092 h nM, half-life 1.12 h). The comprehensive analyzed PK parameters are listed in Figure 4 and Supplemental Figure 2.

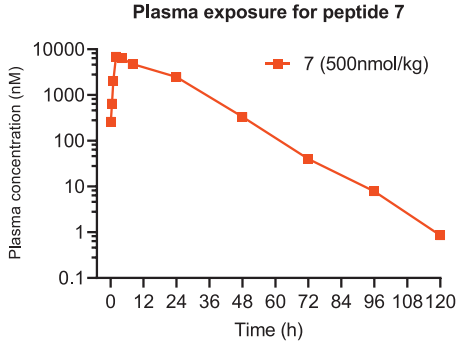

Peptide	$t_{1/2}$ (h)	t_{max} (h)	C_{max} (nmol/L)	AUC_{last} (h*nmol/L)	AUC/Dose (nM*Hours/nmol/kg)
7	8.45	2	6930.0	137272.2	274.54

Figure 4: Pharmacokinetics of the peptide antagonist **7**. Plasma exposure (panel) and pharmacokinetic parameters (table) for peptide **7** dosed at 500 nmol/kg in DIO mice.

3.6. Peptide **7** is effective at blocking both pharmacologic and physiologic GIP action

We validated the *in vivo* antagonistic effect of **7** on both pharmacologic and physiologic GIP action in DIO mice. We treated mice via SC injection with either vehicle, acyl-GIP [27] (1 nmol/kg), **7** (500 nmol/kg or 1500 nmol/kg), or acyl-GIP + **7** (1 nmol/kg + 500 nmol/kg or 1500 nmol/kg) prior to an intraperitoneal glucose tolerance test (IPGTT) to assess the ability of **7** to block exogenous, pharmacologic GIP action on glucose control (Figure 5 A, B). Acyl-GIP significantly reduced glucose excursion during the IPGTT as expected, while **7** alone at both doses had a numeric but insignificant effect to increase glycemia. Pretreatment with **7** caused a dose-dependent negation of the glucose control effect of acyl-GIP (Figure 5 A, B). The combination of the high dose of **7** with acyl-GIP resulted in a glucose excursion profile that is significantly elevated relative to that of acyl-GIP treatment alone and on par with the vehicle controls. Peptide **7** did not affect semaglutide mediated reductions in blood glucose during an IPGTT (Figure 6C,D) oral glucose tolerance test (Supplemental figure 3). Collectively, these data indicate that **7** is sufficient to block pharmacologic GIP action in mice at the doses tested here.

We further assessed the ability of **7** to block endogenous incretin action on glucose control in the context of an oral glucose tolerance test. We injected mice with either vehicle or **7** (500 nmol/kg and 1500 nmol/kg) 1 h prior to an oral gavage of glucose at a dose demonstrated to stimulate endogenous GIP secretion (Figure 5C,D) [30,31]. Pretreatment with the high dose of peptide **7** worsened glucose control in this context, indicating that peptide **7** can antagonize endogenous incretin action in mice in the dose range tested here.

3.7. Peptide **7** potentiates body weight loss when co-administered with a GLP-1R agonist

Emerging data supports that antibody-based GIPR antagonism combined with GLP-1R agonism, results in greater body weight loss in mice

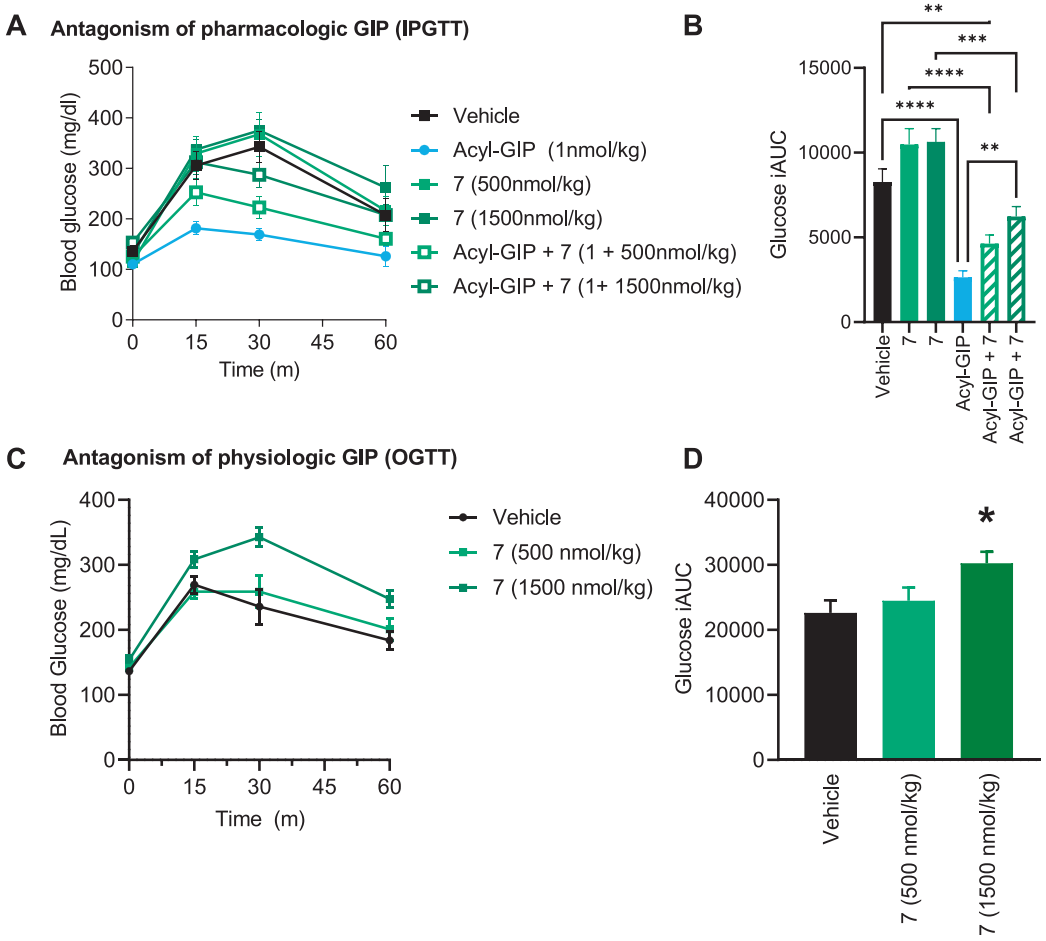

Figure 5: Peptide **7** diminishes the effects of both pharmacologic and physiologic GIP. Blood glucose (A, C) and glucose integrated area under the curve (B, D) during an IPGTT (A, B) and OGTT (B, D) in DIO mce treated with either Acyl-GIP, peptide **7**, or Acyl-GIP + **7**. Data represent mean ± SEM, n = 8 per group. * represents $p < 0.05$, ** represents $p < 0.01$, *** represents $p < 0.001$, **** represents $p < 0.0001$ compared to either vehicle or indicated group).

than what is achieved with GLP-1R agonism alone [9,32,33]. We sought to test whether the GIPR antagonizing peptide **7** can provide similar efficacy when combined with the GLP-1R agonist semaglutide (Figure 6A). Minimal weight change resulted from GIPR antagonist treatment alone (peptide **7** at 500 nmol/kg/d = +2.57% and 1500 nmol/kg/d = −2.88%). The GLP-1R agonist semaglutide (2 nmol/kg/d) produced significant weight reduction (−14.79%) compared to vehicle, as expected. The combination of semaglutide with **7** at both dose levels produced significantly more body weight lowering than semaglutide alone (−22.43% and −27.76%, respectively). Antagonist **7** modestly but dose-dependently lowered food intake (FI; Figure 6B). Semaglutide elicited a greater anorectic effect than GIPR antagonist, while the combination of the GLP-1R agonist with GIPR antagonist displayed the greatest reduction in FI. On day 26 we performed an IPGTT in each group 24 h after compound injection and found that animals treated with semaglutide, semaglutide plus **7**, and **7** alone (500 nmol/kg) all showed significantly improved glucose control compared to controls (Figure 6C,D); the high dose **7** treated animals showed numeric but insignificant lowering of glucose iAUC in this experiment (Figure 6D). While glucose iAUC for the **7** + semaglutide group was not significantly lower than semaglutide alone, the 30 m time point did meet the criteria for significance using a two-way ANOVA (Figure 6C).

Finally, we assessed fasted insulin (Figure 6E) and resistin levels (Figure 6F) to gauge surrogate measures of insulin resistance, and CTX levels as a marker of bone health (Figure 6G) after a 6 h fast on day 27 of treatment. All groups treated with semaglutide showed reductions in fasted insulin compared to vehicle treated controls, consistent with improved insulin sensitivity accompanying weight-loss. Treatment with **7** did not modify reduction in fasting insulin levels seen with semaglutide treatment. No significant changes to resistin were seen in any group. Semaglutide treatment reduced circulating CTX, consistent with improved bone health, while high dose **7** mitigated these gains, in keeping with a potentially deleterious effect of GIPR antagonism on bone density [23,34].

3.8. Peptide **7** antagonizes GIPR but not GLP-1R in islets from human donors

To functionally test the antagonistic properties of **7** in a native human cell system, we perifused intact human islets with either GIP or GLP-1 (Figure 7A,B). There was no difference between treatment groups at high glucose alone for either donor (C, D); native GIP (E, F) and native GLP-1 (G, H) stimulated insulin secretion comparably in two independent sets of human islets. The GIPR antagonist **7** completely inhibited insulin secretion in response to GIP (E, F), but had no impact on the response to GLP-1 (G, H), demonstrating specificity for the GIPR

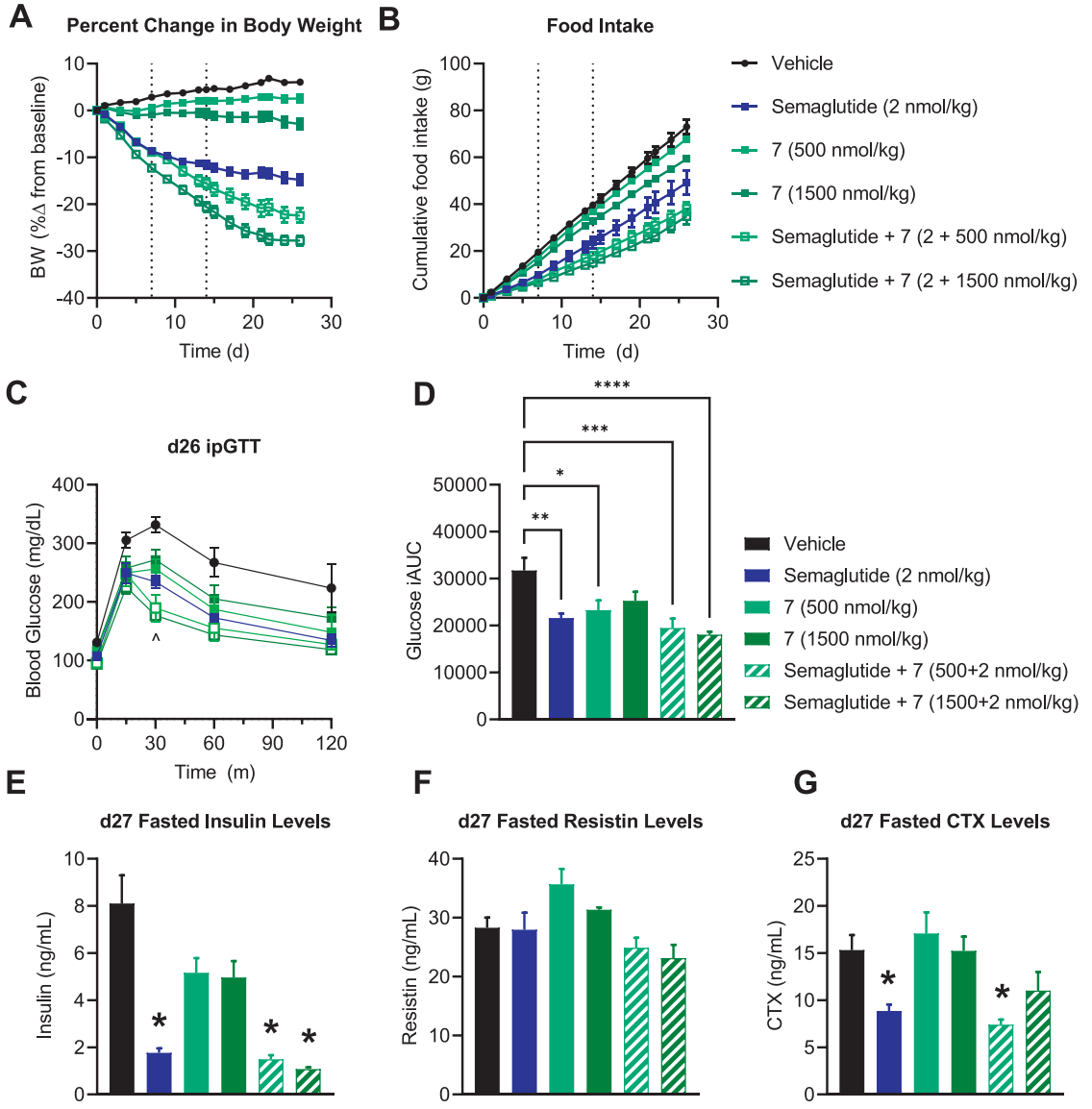

Figure 6: GIPR antagonism via Peptide **7** enhances GLP-1 mediated weight loss. (A) Percent change in body weight and (B) cumulative food intake for DIO mice treated with either semaglutide (2 nmol/kg QD), **7** (500 or 1500 nmol/kg QD), or semaglutide + 7 (2 nmol/kg QD + either 500 or 1500 nmol/kg QD) for 27 d. The blood glucose (A) and glucose iAUC (B) were assessed in an IPGTT on day 26. On day 27 animals were fasted for 6 h and plasma was collected for assessment of (C) insulin, (D) resistin, and (E) CTX. Data represent mean ± SEM, n = 8 per group. * represents $p < 0.05$ compared to either vehicle or indicated group; ^ indicates $p < 0.05$ between semaglutide vs. semaglutide +7 (1500 nmol/kg.

at the doses tested. There is a modest and transient, statistically insignificant rise in insulin secretion in response to the GIPR antagonist alone (C, D) which speaks against any functional ramifications of the hGcgR antagonism seen in the over expressing cell line *in vitro* (Figure 3) and may be indicative of the low potency GLP-1R agonism in compound **7.**

4. DISCUSSION

The paradoxical finding that GIPR agonists and antagonists drive additional weight loss when combined with GLP-1R agonists sits at the forefront of the incretin pharmacology field [35,36]. In fact, the weight loss seen with either an agonist or antagonist appears comparable in DIO mice [9]. Mechanistic explanations for these data are accordingly complex and we will restrict our discussion to four potential hypotheses suggested by the literature. First, preclinical reports that show chronic GIPR agonism drives GIPR desensitization provide a potential unifying link between agonism and antagonism [9]. Second, it may also be possible that GIPR/GLP-1R coexpressing neurons in the hypothalamus [37] are both accessible to large GIPR neutralizing antibodies and display a similar compensatory GLP-1R sensitization as observed in B-cells [38,39] when the GIPR is blocked. Third, central GIPR agonism in preclinical species can mediate weight-loss via reduced food intake, while putatively peripherally restricted GIPR neutralizing antibodies inhibit lipogenesis and promote weight loss. Finally, the recent demonstration that GIPR is expressed in adipose tissue associated pericytes [40] indicates that GIPR agonism may facilitate enhanced blood flow or vascularization

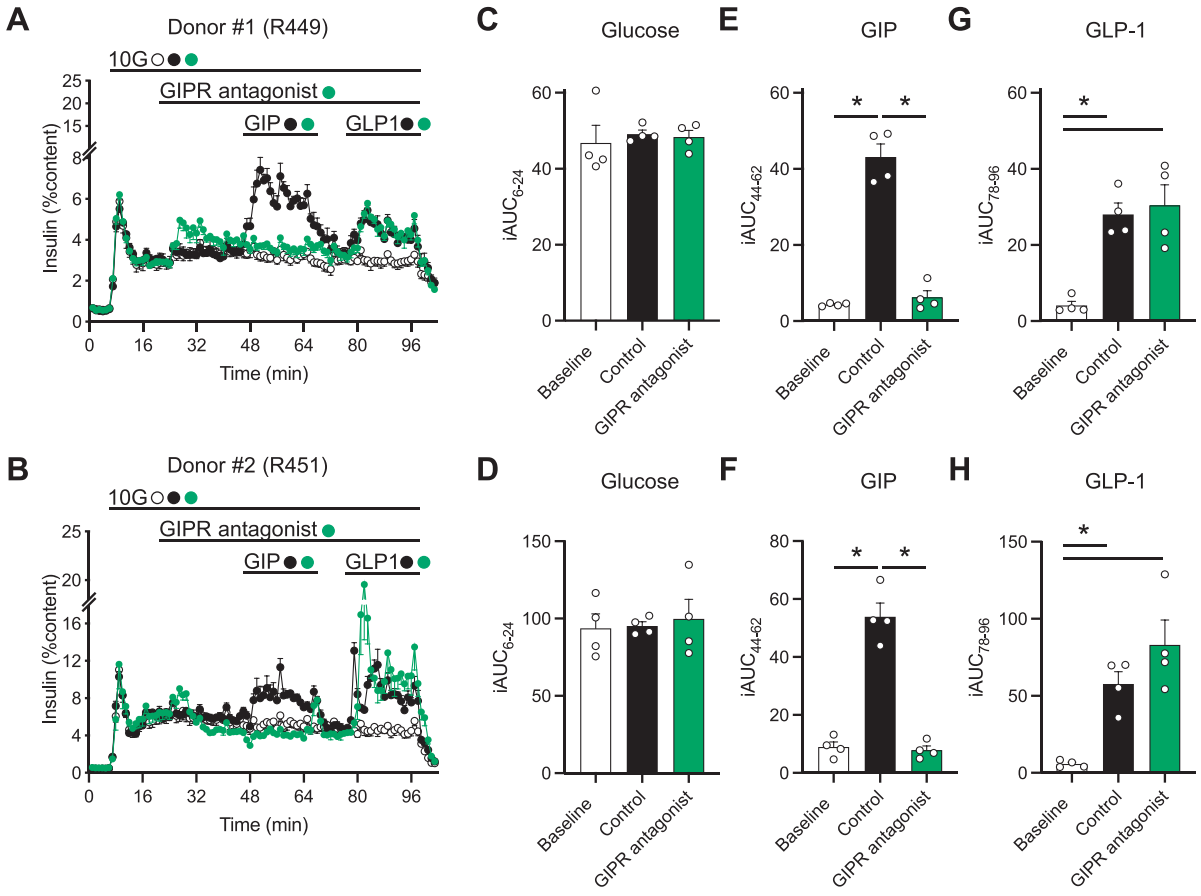

Figure 7: GIPR antagonism via peptide 7 reduces GIP but not GLP-1 stimulated insulin secretion from islets from human donors. Insulin secretion from islets from two human donors (A, R449 and B, R451) was measured in response to glucose, GIP, and GLP-1 ± **7** as indicated. The area under the curve (AUC) for glucose (C, D; 8—24 m), GIP (E, F; 44—62 m), and GLP-1 (G, H; 78—96 m) stimulated insulin secretion is recorded for each individual donor. Data represent mean ± SEM for 4 technical replicates per donor.

to allow GLP-1 biodistribution into anatomical regions that drive weight loss. These pharmacologic data combine with previous reports that GIPR knockout mice are protected from DIO [1,41—43] to indicate a broad but unsatisfying conclusion that pharmacological manipulation of GIPR action plays a critical, yet incompletely defined role in metabolic homeostasis. This has led to the emergence of both GIPR agonizing peptides along with GIPR neutralizing antibodies [32,33] as potential therapeutics for obesity. While GIPR peptide antagonists have been shown to protect against DIO in ovariectomized female mice [14] and provide benefit on glucose homeostasis in preclinical studies [44—46] including our own (Figure 6C,D), the current literature largely reflects an inability of previous GIPR peptide antagonists to produce additive weight reduction in DIO rodents [27,45] or additively modulate appetite and energy expenditure in obese humans when combined with GLP-1R agonists [47]. The lack of efficacy in this regard may be due to differences in mouse models used, relative potency of either GIPR antagonists or GLP-1R agonists, or metabolic liabilities leading to degradation of the peptide antagonist as we demonstrate here (Supplemental figure 2). In this work we present the discovery of a GIPR antagonist that demonstrates efficacy to drive additional body weight loss when coupled with the GLP-1R agonist semaglutide. While the predicted once-daily dosing frequency of this compound makes it unappealing for clinical development, our GIPR antagonist is a useful tool for interrogating the biology of GIP in preclinical and clinical settings.

The truncated peptide $GIP_{(3-30)}$ (**1**) serves as a GIPR inhibitor, potentially by mimicking the interactions of $GIP_{(16-30)}$ [48] with the receptor extracellular domain, but lacking critical residues for signaling activation by $GIP_{(1-15)}$ within the receptor transmembrane domain [49]. In this study, we investigated the potential GIPR antagonism of the truncated sequences $GIP_{(3-30)}$, $GIP_{(5-31)}$ and $GIP_{(6-31)}$ based on our previous work with a $GIP_{(5-42)}$ fragment [27]. We sought to enhance the antagonistic efficacy of the GIP truncated peptides through a series of mutations to the peptide backbone and the incorporation fatty acid-based protractors. A His18/Arg mutation borrowed from the mGIP sequence was incorporated to enhance antagonism at the mGIPR based on our previously reported optimization of GIPR agonists [27]. The Met14/Leu substitution was selected to avoid predicted proteolytic cleavage while the Asp21/Glu mutation was incorporated to improve molecular physiochemical properties. The N-terminus acetylic capping was performed to lower the acidic pI and improve solubility in neutral pH buffers compared to C-terminal amide containing compounds. These mutations provided only mildly enhanced inhibition at the hGIPR in peptides **2**, **3, 4** and **5**, as expected, but offered considerably more potency at the mGIPR compared to **1**. Finally, we incorporated Pla at position 6 based on our previous work with glucagon receptor antagonists [50] and may serve to diminish conformational changes in the transmembrane orthosteric binding domain that are critical for receptor activation [25]. However, this is speculative. While **5** proved the most potent antagonist among the non-acylated peptides, its

acylated iteration **8** was unexpectedly less potent than **7**, an acylated iteration of **3**. This demonstrates that fatty acid protractors do not merely drive extensions in half-life, but also are active contributors to the pharmacophore, in keeping with our previous report of optimized GIPR agonists [27]. The nature of this improved pharmacology is unknown but potential explanations include a direct interaction for the acylation with the receptor or an anchoring effect of the acylation to the cell membrane which facilitates receptor:compound interaction. We attempted to further optimize the time-action of **7** by replacing the C16 monoacid acylation with a C18 diacid acylation with various linkers (**9, 10** and **11**). However, these diacid protractor substitutions analgouse to those seen in the GLP-1R agonist semaglutide all reduced antagonistic potency, further speaking to the potential interactions of C16 monacid acylation with the GIPR. We also demonstrated that acylation at position 11 is superior to position 10, as **7** displayed improved antagonism on mGIPR cAMP signals compared to **12** and **13**.

The cAMP generation assay data referenced above generally rank orders the compounds similarly to the *in vitro* receptor binding assay (Table 1). However, some discrepancies exist. It is plausible that discordance between the two assays is due to the over expression of receptors and amplification of cAMP signal in the cAMP assay. These facets of the assay provide greater discrimination between compounds at lower doses. We have tried to synchronize interpretations of both assays to select compounds for further investigation and find that **7** provides optimal GIPR antagonism across assays without exhibiting residual GIPR agonism or imparting substantial GLP-1R cross reactivity. Truncated peptide antagonists frequently suffer from a lack of specificity at closely related receptors. We tested the cross reactivity of **7** at the GLP-1R and found that 7 demonstrated limited agonism for either the hGLP-1R, mGLP-1R, hGcgR, or mGcgR but did show low potency, high efficacy antagonism of hGLP-1R and hGcgR respectively. While this concern should be noted, the demonstration that **7** does not mitigate GLP-1 mediated insulin secretion nor does it enhance glucose stimulated insulin secretion alone in intact human islets indicates a sufficient window for GIPR antagonism without GLP-1R or GcgR antagonism. This speaks to the limitations of receptor overexpressing cell lines to inidicate functional outcomes in native systems with relatively lower receptor abundance. These *in vitro* assays are useful for rank ordering compounds but should not be assumed to reflect the dynamics of physiologic systems.

We previously reported a $GIP_{(5\text{-}42)}$ peptide antagonist with palmitoylation at position 10 ([N^{α}-Ac, L14, R18, E21]$hGIP_{(5\text{-}42)}$-K10 (γEγE-C16), **13** in the present work) exhibits potent antagonism at both hGIPR and mGIPR. However, peptide **13** did not improve weight loss when co-administrated with the GLP-1R agonist liraglutide in DIO mice [27]. Subsequently, a similar peptide antagonist which removed the Met14/Leu and Asp21/Glu mutations in **13** was reported to be unable to enhance the body weight lowering of liraglutide in mice [27]. In the present studies, we sought to address why **13** did not function as well as **7** in this respect. First, peptide **13** is ∼5-fold less potent at mGIPR than **7** *in vitro*. Second, and perhaps most critically, our PK analysis demonstrates a kinetic liability in **13** that results in a substantially longer half-life and elevated maximal concentration of **7** compared to **13**. These data indicate that the PK profile and physiochemical properties of **7** are superior to **13**, rendering it more suitable for chronic *in vivo* studies in mice.

In summary, we describe the discovery of potent peptide GIPR antagonists. The peptide antagonists were characterized and validated by cAMP signaling and receptor binding assays *in vitro*. The mouse *in vivo* pharmacology was conducted with the lead palmitoylated $GIP_{(5\text{-}31)}$ analogue **7**, which proved effective at blocking both pharmacologic and physiologic GIP in an *in vivo* setting in DIO mice. Furthermore, daily coadministration of **7** with the GLP-1R agonist semaglutide resulted in potentiated body weight reductions in DIO mice, the first demonstration of this kind with a GIPR peptide antagonist. Peptide **7** effectively blocked GIP action in native human islets. The speculations as to whether the GIPR antagonists or antibodies will emerge as clinical candidates is unknown, however the peptide antagonists described in this manuscript may prove to be a useful tool compound to better understanding the role of GIP in metabolic homeostasis.

AUTHOR CONTRIBUTIONS

B.Y. designed and synthesized peptides, assisted *in vitro* assays, interpreted experimental results, and co-wrote the manuscript. V.M.G. assembled, validated, and conducted the *in vitro* cAMP bioassay, interpreted results, and co-wrote the manuscript. R.R. and B.D. conducted PK measurements, interpreted the results, and cowrote the manuscript. A.M.K.H conducted the receptor binding assay, interpreted the results, and cowrote the manuscript. K.E, A.C, D.D.A and J.E.C conducted the human islet perifusion experiments, interpreted the results, and cowrote the manuscript. P.J.K. interpreted results, and cowrote the manuscript. D.P.T. performed the *in vivo* pharmacology, interpreted the results, and cowrote the manuscript. J.D.D. conceptualized the *in vivo* pharmacology studies, interpreted the results, co-wrote and edited the manuscript. B.F. conceptualized the project, interpreted results and edited the manuscript.

DATA AVAILABILITY

Data will be made available on request.

ACKNOWLEDGMENTS

The authors extend our sincere thanks to the donors of the islets used in these studies for their dedication and contribution to scientific advancement. The authors also thanks for Jay Levy assistant synthesized peptides, Catharina Dreijer Sørensen and Vibeke Nielsen conducted the receptor binding assay, University of Cincinnati scientists for conducting *in vivo* pharmacology studies. Additionally, thanks for Drs. Richard DiMarchi and Jesper Lau for having supported the project. Research funding was provided by Novo Nordisk.

CONFLICTS OF INTEREST

The authors declare the following authors B.Y., V.M.G., R.R., B.D., A.M.K.H., P.J.K., J.D.D., and B.F. are currently Novo Nordisk employees. J.E.C., D.A.D., and D.P.T. receive funding from Novo Nordisk.

APPENDIX A. SUPPLEMENTARY DATA

Supplementary data to this article can be found online at https://doi.org/10.1016/j.molmet.2022.101638.

REFERENCES

[1] Miyawaki, K., Yamada, Y., Ban, N., Ihara, Y., Tsukiyama, K., Zhou, H., et al., 2002. Inhibition of gastric inhibitory polypeptide signaling prevents obesity. Nat Med 8(7):738–742.

[2] Ayala, J.E., Bracy, D.P., James, F.D., Burmeister, M.A., Wasserman, D.H., Drucker, D.J., 2010. Glucagon-like peptide-1 receptor knockout mice are protected from high-fat diet-induced insulin resistance. Endocrinology 151(10): 4678–4687.

[3] Hansotia, T., Maida, A., Flock, G., Yamada, Y., Tsukiyama, K., Seino, Y., et al., 2007. Extrapancreatic incretin receptors modulate glucose homeostasis, body weight, and energy expenditure. J Clin Invest 117(1):143—152.

[4] Zhang, Q., Delessa, C.T., Augustin, R., Bakhti, M., Collden, G., Drucker, D.J., et al., 2021. The glucose-dependent insulinotropic polypeptide (GIP) regulates body weight and food intake via CNS-GIPR signaling. Cell Metabol 33(4):833—844.

[5] Frias, J.P., Nauck, M.A., Van, J., Benson, C., Bray, R., Cui, X., et al., 2020. Efficacy and tolerability of tirzepatide, a dual glucose-dependent insulinotropic peptide and glucagon-like peptide-1 receptor agonist in patients with type 2 diabetes: a 12-week, randomized, double-blind, placebo-controlled study to evaluate different dose-escalation regimens. Diabetes Obes Metabol 22(6):938—946.

[6] Min, T., Bain, S.C., 2021. The role of tirzepatide, dual GIP and GLP-1 receptor agonist, in the management of type 2 diabetes: the SURPASS clinical trials. Diabetes Ther 12(1):143—157.

[7] Frias, J.P., Davies, M.J., Rosenstock, J., Perez Manghi, F.C., Fernandez Lando, L., Bergman, B.K., et al., 2021. Tirzepatide versus semaglutide once weekly in patients with type 2 diabetes. N Engl J Med 385:503—515.

[8] Schmitt, C., Portron, A., Jadidi, S., Sarkar, N., DiMarchi, R., 2017. Pharmacodynamics, pharmacokinetics and safety of multiple ascending doses of the novel dual glucose-dependent insulinotropic polypeptide/glucagon-like peptide-1 agonist RG7697 in people with type 2 diabetes mellitus. Diabetes Obes Metabol 19(10):1436—1445.

[9] Killion, E.A., Chen, M., Falsey, J.R., Sivits, G., Hager, T., Atangan, L., et al., 2020. Chronic glucose-dependent insulinotropic polypeptide receptor (GIPR) agonism desensitizes adipocyte GIPR activity mimicking functional GIPR antagonism. Nat Commun 11(1):4981.

[10] Killion, E.A., Wang, J., Yie, J., Shi, S.D.-H., Bates, D., Min, X., et al., 2018. Anti-obesity effects of GIPR antagonists alone and in combination with GLP-1R agonists in preclinical models. Sci Transl Med 10:1—11.

[11] Baggio, L.L., Kim, J.G., Drucker, D.J., 2004. Chronic exposure to GLP-1R agonists promotes homologous GLP-1 receptor desensitization in vitro but does not attenuate GLP-1R-dependent glucose homeostasis in vivo. Diabetes 53(Suppl 3):S205—S214.

[12] Hansen, L.S., Sparre-Ulrich, A.H., Christensen, M., Knop, F.K., Hartmann, B., Holst, J.J., et al., 2016. N-terminally and C-terminally truncated forms of glucose-dependent insulinotropic polypeptide are high-affinity competitive antagonists of the human GIP receptor. Br J Pharmacol 173(5):826—838.

[13] Perry, R.A., Craig, S.L., Ng, M.T., Gault, V.A., Flatt, P.R., Irwin, N., 2019. Characterisation of glucose-dependent insulinotropic polypeptide receptor antagonists in rodent pancreatic beta cells and mice. Clin Med Insights Endocrinol Diabetes 12:1179551419875453.

[14] Pathak, V., Gault, V.A., Flatt, P.R., Irwin, N., 2015. Antagonism of gastric inhibitory polypeptide (GIP) by palmitoylation of GIP analogues with N- and C-terminal modifications improves obesity and metabolic control in high fat fed mice. Mol Cell Endocrinol 401:120—129.

[15] Boer, G.A., Hunt, J.E., Gabe, M.B.N., Windelov, J.A., Sparre-Ulrich, A.H., Hartmann, B., et al., 2022. Glucose-dependent insulinotropic polypeptide receptor antagonist treatment causes a reduction in weight gain in ovariectomised high fat diet-fed mice. Br J Pharmacol 179(18):4486—4499.

[16] Sparre-Ulrich, A.H., Hansen, L.S., Svendsen, B., Christensen, M., Knop, F.K., Hartmann, B., et al., 2016. Species-specific action of (Pro3)GIP - a full agonist at human GIP receptors, but a partial agonist and competitive antagonist at rat and mouse GIP receptors. Br J Pharmacol 173(1):27—38.

[17] Gault, V.A., O'Harte, F.P., Harriott, P., Mooney, M.H., Green, B.D., Flatt, P.R., 2003. Effects of the novel (Pro3)GIP antagonist and exendin(9-39)amide on GIP- and GLP-1-induced cyclic AMP generation, insulin secretion and postprandial insulin release in obese diabetic (ob/ob) mice: evidence that GIP is the major physiological incretin. Diabetologia 46(2):222—230.

[18] Deacon, C.F., 2004. Circulation and degradation of GIP and GLP-1. Horm Metab Res 36(11—12):761—765.

[19] Deacon, C.F., Plamboeck, A., Rosenkilde, M.M., de Heer, J., Holst, J.J., 2006. GIP-(3-42) does not antagonize insulinotropic effects of GIP at physiological concentrations. Am J Physiol Endocrinol Metab 291(3):E468—E475.

[20] Kerr, B.D., Flatt, A.J., Flatt, P.R., Gault, V.A., 2011. Characterization and biological actions of N-terminal truncated forms of glucose-dependent insulinotropic polypeptide. Biochem Biophys Res Commun 404(3):870—876.

[21] Sparre-Ulrich, A.H., Gabe, M.N., Gasbjerg, L.S., Christiansen, C.B., Svendsen, B., Hartmann, B., et al., 2017. GIP(3-30)NH2 is a potent competitive antagonist of the GIP receptor and effectively inhibits GIP-mediated insulin, glucagon, and somatostatin release. Biochem Pharmacol 131:78—88.

[22] Gabe, M.B.N., Sparre-Ulrich, A.H., Pedersen, M.F., Gasbjerg, L.S., Inoue, A., Brauner-Osborne, H., et al., 2018. Human GIP(3-30)NH2 inhibits G protein-dependent as well as G protein-independent signaling and is selective for the GIP receptor with high-affinity binding to primate but not rodent GIP receptors. Biochem Pharmacol 150:97—107.

[23] Gasbjerg, L.S., Hartmann, B., Christensen, M.B., Lanng, A.R., Vilsboll, T., Jorgensen, N.R., et al., 2020. GIP's effect on bone metabolism is reduced by the selective GIP receptor antagonist GIP(3-30)NH2. Bone 130:115079.

[24] Knerr, P.J., Mowery, S.A., Douros, J.D., Premdjee, B., Hjollund, K.R., He, Y., et al., 2022. Next generation GLP-1/GIP/glucagon triple agonists normalize body weight in obese mice. Mol Metabol 63:101533.

[25] Yang, B., Gelfanov, V.M., Perez-Tilve, D., DuBois, B., Rohlfs, R., Levy, J., et al., 2021. Optimization of truncated glucagon peptides to achieve selective, high potency, full antagonists. J Med Chem 64(8):4697—4708.

[26] Lynggaard, M.B., Gasbjerg, L.S., Christensen, M.B., Knop, F.K., 2020. GIP(3-30)NH2 - a tool for the study of GIP physiology. Curr Opin Pharmacol 55:31—40.

[27] Mroz, P.A., Finan, B., Gelfanov, V., Yang, B., Tschop, M.H., DiMarchi, R.D., et al., 2019. Optimized GIP analogs promote body weight lowering in mice through GIPR agonism not antagonism. Mol Metabol 20:51—62.

[28] Capozzi, M.E., Svendsen, B., Encisco, S.E., Lewandowski, S.L., Martin, M.D., Lin, H., et al., 2019. Beta Cell tone is defined by proglucagon peptides through cAMP signaling. JCI Insight 4(5).

[29] Lau, J., Bloch, P., Schaffer, L., Pettersson, I., Spetzler, J., Kofoed, J., et al., 2015. Discovery of the once-weekly glucagon-like peptide-1 (GLP-1) analogue semaglutide. J Med Chem 58(18):7370—7380.

[30] Douros, J.D., Niu, J., Sdao, S., Gregg, T., Merrins, M.J., Campbell, J., et al., 2019. Temporal plasticity of insulin and incretin secretion and insulin sensitivity following sleeve gastrectomy contribute to sustained improvements in glucose control. Mol Metabol 28:144—150.

[31] Douros, J.D., Niu, J., Sdao, S., Gregg, T., Fisher-Wellman, K., Bharadwaj, M., et al., 2019. Sleeve gastrectomy rapidly enhances islet function independently of body weight. JCI Insight 4(6).

[32] Killion, E.A., Wang, J., Yie, J., Shi, S.D., Bates, D., Min, X., et al., 2018. Anti-obesity effects of GIPR antagonists alone and in combination with GLP-1R agonists in preclinical models. Sci Transl Med 10(472).

[33] Lu, S.C., Chen, M., Atangan, L., Killion, E.A., Komorowski, R., Cheng, Y., et al., 2021. GIPR antagonist antibodies conjugated to GLP-1 peptide are bispecific molecules that decrease weight in obese mice and monkeys. Cell Rep Med 2(5):100263.

[34] Vyavahare, S.S., Mieczkowska, A., Flatt, P.R., Chappard, D., Irwin, N., Mabilleau, G., 2020. GIP analogues augment bone strength by modulating bone composition in diet-induced obesity in mice. Peptides 125:170207.

[35] Knerr, P.J., Mowery, S.A., Finan, B., Perez-Tilve, D., Tschop, M.H., DiMarchi, R.D., 2020. Selection and progression of unimolecular agonists at the GIP, GLP-1, and glucagon receptors as drug candidates. Peptides 125:170225.

[36] Holst, J.J., 2021. What combines best with GLP-1 for obesity treatment: GIP receptor agonists or antagonists? Cell Rep Med 2(5):100284.

[37] Adriaenssens, A.E., Biggs, E.K., Darwish, T., Tadross, J., Sukthankar, T., Girish, M., et al., 2019. Glucose-dependent insulinotropic polypeptide receptor-expressing cells in the hypothalamus regulate food intake. Cell Metabol 30(5):987–996 e986.

[38] Campbell, J.E., Ussher, J.R., Mulvihill, E.E., Kolic, J., Baggio, L.L., Cao, X., et al., 2016. TCF1 links GIPR signaling to the control of beta cell function and survival. Nat Med 22(1):84–90.

[39] Pamir, N., Lynn, F.C., Buchan, A.M.J., Ehses, J., Hinke, S.A., Pospisilik, J.A., et al., 2003. Glucose-dependent insulinotropic polypeptide receptor null mice exhibit compensatory changes in the enteroinsular axis. Am J Physiol Endocrinol Metab 284:E931–E939.

[40] Campbell, J.E., Beaudry, J.L., Svendsen, B., Baggio, L.L., Gordon, A.N., Ussher, J.R., et al., 2022. GIPR is predominantly localized to nonadipocyte cell types within white adipose tissue. Diabetes 71(5):1115–1127.

[41] Yabe, D., Seino, Y., 2013. Incretin actions beyond the pancreas: lessons from knockout mice. Curr Opin Pharmacol 13(6):946–953.

[42] Asmar, M., Asmar, A., Simonsen, L., Gasbjerg, L.S., Sparre-Ulrich, A.H., Rosenkilde, M.M., et al., 2017. The gluco- and liporegulatory and vasodilatory effects of glucose-dependent insulinotropic polypeptide (GIP) are abolished by an antagonist of the human GIP receptor. Diabetes 66(9):2363–2371.

[43] Jones, I.R., Owens, D.R., Vora, J., Luzio, S.D., Hayes, T.M., 1989. A supplementary infusion of glucose-dependent insulinotropic polypeptide (GIP) with a meal does not significantly improve the beta cell response or glucose tolerance in type 2 diabetes mellitus. Diabetes Res Clin Pract 7(4):263–269.

[44] Pathak, V., Vasu, S., Gault, V.A., Flatt, P.R., Irwin, N., 2015. Sequential induction of beta cell rest and stimulation using stable GIP inhibitor and GLP-1 mimetic peptides improves metabolic control in C57BL/KsJ db/db mice. Diabetologia 58(9):2144–2153.

[45] West, J.A., Tsakmaki, A., Ghosh, S.S., Parkes, D.G., Gronlund, R.V., Pedersen, P.J., et al., 2021. Chronic peptide-based GIP receptor inhibition exhibits modest glucose metabolic changes in mice when administered either alone or combined with GLP-1 agonism. PLoS One 16(3):e0249239.

[46] Irwin, N., McClean, P.L., Hunter, K., Flatt, P.R., 2009. Metabolic effects of sustained activation of the GLP-1 receptor alone and in combination with background GIP receptor antagonism in high fat-fed mice. Diabetes Obes Metabol 11(6):603–610.

[47] Stensen, S., Krogh, L.L., Sparre-Ulrich, A.H., Dela, F., Hartmann, B., Vilsboll, T., et al., 2022. Acute concomitant glucose-dependent insulinotropic polypeptide receptor antagonism during glucagon-like peptide 1 receptor agonism does not affect appetite, resting energy expenditure or food intake in patients with type 2 diabetes and overweight/obesity. Diabetes Obes Metabol 24(9):1882–1887.

[48] Parthier, C., Kleinschmidt, M., Neumann, P., Rudolph, R., Manhart, S., Schlenzig, D., et al., 2007. Crystal structure of the incretin-bound extracellular domain of a G protein-coupled receptor. Proc Natl Acad Sci U S A 104(35):13942–13947.

[49] Smit, F.X., van der Velden, W.J.C., Kizilkaya, H.S., Norskov, A., Luckmann, M., Hansen, T.N., et al., 2021. Investigating GIPR (ant)agonism: a structural analysis of GIP and its receptor. Structure 29(7):679–693 e676.

[50] Yang, B., Gelfanov, V.M., Perez-Tilve, D., DuBois, B., Rohlfs, R., Levy, J., et al., 2021. Optimization of truncated glucagon peptides to achieve selective, high potency, full antagonists. J Med Chem 64(8):4697–4708.

